Synthesis of Potassium Niobate (KNbO₃) Thin Films by Low-Temperature Hydrothermal Epitaxy

Wojciech L. Suchanek

Sawyer Research Products, Inc., 35400 Lakeland Boulevard, Eastlake, Ohio 44095

Orthorhombic $KNbO_3$ thin films were deposited on $SrTiO_3$ (100) and $LiTaO_3$ (001) substrates by low-temperature hydrothermal epitaxy at 180−210 °C using aqueous solutions containing Nb_2O_5 and KOH. The films were thoroughly characterized by X-ray diffraction, Rutherford backscattering, and scanning electron microscopy. The $KNbO_3$ films were uniformly distributed on the entire substrate area, exhibited high stoichiometry, and did not show evidence of interdiffusion or chemical reaction at the film/substrate interface. Their microstructures were determined by the substrate used, the synthesis temperature, and the concentration of the reactants. The $KNbO_3$ films on $SrTiO_3$ (100) substrates with thickness of 45 nm to 1.28 μm were smooth and transparent, with microstructures strongly suggesting single crystal growth mechanism. They were pure orthorhombic phase with (011) orientation and probably single-domain. Conversely, the $KNbO_3$ films with higher thickness (>3.5 μm) exhibited very rough microstructure with textured columnar grains. Such films were also orthorombic but with mixed (100)/(011) orientation. This work demonstrated for the first time deposition of heteroepitaxial $KNbO_3$ films on single-crystal substrates using low-temperature hydrothermal epitaxy in a well-defined range of synthesis conditions. The low synthesis temperatures, which are below the 225 °C phase transition temperature of $KNbO_3$, resulted in formation of films that appear to exhibit improved features as compared to the films prepared by high-temperature processing.

Introduction

Potassium niobate ($KNbO_3$) is a very promising material for surface acoustic wave (SAW) devices and high-performance bulk-wave transducers.[1] The electromechanical coupling coefficient (k^2) of the surface wave in a single-crystal $KNbO_3$ can be as high as 53%, which is one order of magnitude larger than that of $LiNbO_3$.[2] The bandwidth is about 20% and insertion losses are 2−6 dB.[2] The acoustic wave velocities in $KNbO_3$ are 3500−7500 m/s [3] and the temperature coefficient of frequency (TCF) ranges between 0 and 170 ppm/K depending upon crystallographic orientation.[2] The $KNbO_3$ exhibits large piezoelectric nonlinearity. The 45° rotated Y-cut X-propagated $KNbO_3$ has 25 dB larger efficiency than Y−Z $LiNbO_3$; thus the $KNbO_3$ single crystal is considered as a promising material for SAW elastic convolvers with super high efficiency and process gain.[4] In addition to excellent piezoelectric properties, the $KNbO_3$ has a large electrooptic coefficient, high nonlinear optical coefficient, and excellent photorefractive characteristics[5] that make it a very promising candidate for optical applications such as optical waveguides, frequency doublers,[6] intensity modulators,[7] optical switching and modifiable interconnections,[7] and holographic storage systems.[8]

Unfortunately, $KNbO_3$ melts incongruently and crystallizes cubic perovskite-type structure, which undergoes two phase transformations during cooling: cubic to tetragonal at 435 °C and tetragonal to orthorhombic at 225 °C.[6] This behavior makes it very difficult to obtain large, crack-free, single-domain crystals. For these reasons, $KNbO_3$ films have been investigated on a variety of substrates as very promising candidates for both optical and frequency control applications. $KNbO_3$ thin films offer several advantages over bulk single crystals of the same material, such as improved compositional control and the ability to utilize low growth rates,[9] in addition to being cheaper and more easily obtainable on low-cost commercial substrates.[10] For electrooptic applications, thin films of $KNbO_3$ feature lower driving voltages and higher modulation speeds than bulk single crystals; moreover, they have the potential for monolithic integration.[11] For SHG applications of optical waveguides, utilization of $KNbO_3$ thin films is preferable over bulk single crystals because of the high cost of $KNbO_3$ large single crystals and

(1) Yamanouchi, K.; Odagawa, H.; Kojima, T.; Onoe, A.; Yoshida, A.; Chikuma, K. *Electron. Lett.* **1998,** *34,* 702.

(2) Yamanouchi, K.; Odagawa, H. *IEEE Trans. Ultrason., Ferroelectrics, Frequency Control* **1999,** *46,* 700.

(3) Zaitsev, B. D.; Kuznetsova, I. E.; Borodina, I. A.; Joshi, S. G. *Ultrasonics* **2001,** *39,* 51.

(4) Cho, Y.; Oota, N.; Odagawa, H.; Yamanouchi, K. *J. Appl. Phys.* **2000,** *87,* 3457.

(5) Wu, X.; Looser, H.; Wuest, H.; Arend, H. *J. Cryst. Growth* **1986,** *78,* 431.

(6) Fukuda, T.; Uematsu, Y. *Jpn. J. Appl. Phys.* **1972,** *11,* 163.

(7) Kip, D. *Appl. Phys. B* **1998,** *67,* 131.

(8) Wang, J. Y.; Guan, Q. C.; Wei, J. Q.; Wang, M.; Liu, Y. G. *J. Cryst. Growth* **1992,** *116,* 27.

(9) Graettinger, T. M.; Rou, S. H.; Ameen, M. S.; Auciello, O.; Kingon, A. I. *Appl. Phys. Lett.* **1991,** *58,* 1964.

(10) Beckers, L.; Buchal, C.; Fluck, D.; Pliska, T.; Gunter, P. *Mater. Sci. Eng. A* **1998,** *253,* 292.

(11) Hoerman, B. H.; Nichols, B. M.; Nystrom, M. J.; Wessels, B. W. *Appl. Phys. Lett.* **1999,** *75,* 2707.

technological difficulties in forming in them waveguides by ion implantation, diffusion, or ion exchange.[12] The main factors for pursuing thin films in acoustic wave applications are a general miniaturization trend in electronic devices using SAW and BAW elements,[13] and the task of SAW suppliers is to integrate as many external functions as possible into the SAW components.[14] Another important factor in realizing the thin films approach is a possibility of enhancing almost all properties of SAW or BAW devices by designing appropriate film/substrate materials or even multilayered thin film structures. Subsequently, all essential properties can be tailored in wide ranges by using different combinations of materials, crystallographic orientations (cuts), and microstructures.[15]

So far, $KNbO_3$ thin films can be synthesized by the following methods: metalorganic chemical vapor deposition (MOCVD),[16–19] pulsed-laser deposition,[10,20–25] sputtering,[26,27] liquid-phase epitaxy,[28–30] and sol–gel.[31–33] All these synthesis routes share similar disadvantages of high-temperature processing, requiring temperatures ranging between 600 °C and over 900 °C to obtain a crystalline $KNbO_3$ phase. The high synthesis temperatures cause typical problems such as difficulties to control potassium stoichiometry due to high volatilization of potassium oxide, interdiffusion between film and the substrate,[20,21,24] formation of interphase layers (particularly in the case of using MgO substrate),[21,24] and multidomain formation during cooling to room temperature.[16,20–23,27,29,30] The presence of pyrochlore and/or amorphous phases, as well as porosity, was

reported particularly for the $KNbO_3$ films synthesized by the sol–gel method.[32,33] In addition, liquid-phase epitaxy (LPE) is not well suited for films with thickness under 1 μm.[30]

In other words, all previously used methods to synthesize $KNbO_3$ films yielded films with more or less deteriorated properties due to the high synthesis temperatures. Therefore, development of a low-temperature fabrication of $KNbO_3$ thin films, particularly at temperatures lower than the tetragonal to orthorhombic phase transformation of 225 °C appears to be necessary in order to realize multiple potential applications of the $KNbO_3$ films. Low-temperature hydrothermal techniques offer such possibilities. Several reports on low-temperature (30–285 °C) hydrothermal synthesis of $KNbO_3$ powders appeared recently in the literature,[34–38] indicating potential for hydrothermal synthesis of $KNbO_3$ thin films. Several attempts to grow thin films of $KNbO_3$ or related compounds by the hydrothermal techniques were also reported. Komatsu et al. unsuccessfully attempted homoepitaxial growth of $KNbO_3$ on a multidomain $KNbO_3$ single crystal with polished pseudocubic {100} planes.[37] The deposit from the surface of the $KNbO_3$ single crystal was identified by X-ray diffraction as a mixture of an amorphous phase and orthorhombic $KNbO_3$ crystals with random orientation. The coating had multiple cracks and did not provide complete surface coverage.[37] Wu et al.[39,40] reported hydrothermal–electrochemical synthesis of thin films of a related material, $K_2Ta_2O_6$, with a pyrochlore structure. The pyrocholore $K_2Ta_2O_6$ films were polycrystalline with a random orientation. However, no perovskite $KTaO_3$ phase could be obtained under these conditions.[39,40] Lange et al. reported synthesis of epitaxial $KTaO_3$ films by low-temperature hydrothermal epitaxy at 175 °C.[41]

The objective of this work was to synthesize orthorhombic $KNbO_3$ films with a single crystallographic orientation and hopefully also single-domain, on such single-crystal substrates as $SrTiO_3$ (100) and $LiTaO_3$ (001) by hydrothermal epitaxy at about 200 °C, i.e., below the phase-transition temperature of 225 °C. The technique used was the low-temperature hydrothermal epitaxy developed originally by Lange,[42] which was successfully applied to synthesize other epitaxial oxide films, such as $BaTiO_3$,[43] $PbTiO_3$,[44] and PZT,[45–47] etc.

(12) Chow, A. F.; Lichtenwalner, D. J.; Auciello, O.; Kingon, A. I.; Busch, J. R.; Wood, V. E. *J. Appl. Phys.* **1995**, *78*, 435.
(13) Su, Q.-X.; Kirby, P.; Komuro, E.; Imura, M.; Zhang, Q.; Whatmore, R. *IEEE Trans. Microwave Theory Tech.* **2001**, *49*, 769.
(14) Meier, H.; Baier, T.; Riha, G. *IEEE Trans. Microwave Theory Tech.* **2001**, *49*, 743.
(15) Hickernell, F. S. *Int. J. High Speed Electron. Syst.* **2000**, *10*, 603.
(16) Nystrom, M. J.; Wessels, B. W.; Chen, J.; Marks, T. J. *Appl. Phys. Lett.* **1996**, *68*, 761.
(17) Onoe, A.; Yoshida, A.; Chikuma, K. *Appl. Phys. Lett.* **1996**, *69*, 167.
(18) Onoe, A.; Yoshida, A.; Chikuma, K. *Appl. Phys. Lett.* **2001**, *78*, 49.
(19) Chattopadhyay, S.; Nichols, B. M.; Hwang, J. H.; Mason, T. O.; Wessels, B. W. *J. Mater. Res.* **2002**, *17*, 275.
(20) Hung, L. S.; Bosworth, L. A. *Appl. Phys. Lett.* **1993**, *62*, 2625.
(21) Zaldo, C.; Gill, D. S.; Eason, R. W.; Mendiola, J.; Chandler, P. J. *Appl. Phys. Lett.* **1994**, *65*, 502.
(22) Gopalan, V.; Raj, R. *J. Am. Ceram. Soc.* **1995**, *78*, 1825.
(23) Christen, H. M.; Boatner, L. A.; Budai, J. D.; Chisholm, M. F.; Gea, L. A.; Marrero, P. J.; Norton, D. P. *Appl. Phys. Lett.* **1996**, *68*, 1488.
(24) Martin, M. J.; Alfonso, J. E.; Mendiola, J.; Zaldo, C.; Gill, D. S.; Eason, R. W.; Chandler, P. J. *J. Mater. Res.* **1997**, *12*, 2699.
(25) Zhang, D. M.; Li, Z. H.; Zhang, M. J.; Wang, X. D.; Huang, M. T.; Yu, B. M.; Xu, D. S.; Wang, Y. M. *Am. Ceram. Soc. Bull.* **2001**, *80*, 57.
(26) Thöny, S. S.; Lehmann, H. W.; Gunter, P. *Appl. Phys. Lett.* **1992**, *61*, 373.
(27) Chow, A. F.; Lichtenwalner, D. J.; Woolcott, R. R.; Graettinger, T. M.; Auciello, O.; Kingon, A. I.; Boatner, L. A.; Parikh, N. R. *Appl. Phys. Lett.* **1994**, *65*, 1073.
(28) Khachaturyan, O. A.; Madoyan, R. S. *Cryst. Res. Technol.* **1984**, *19*, 461.
(29) Hulliger, J.; Gutman, R.; Wuest, H. *J. Cryst. Growth* **1993**, *128*, 897.
(30) Gutmann, R.; Hulliger, J.; Reusser, E. *J. Cryst. Growth* **1993**, *126*, 578.
(31) Nazeri-Eshghi, A.; Kuang, A. X.; Mackenzie, J. D. *J. Mater. Sci.* **1990**, *25*, 3333.
(32) Nazeri, A.; Kahn, M. *J. Am. Ceram. Soc.* **1992**, *75*, 2125.
(33) Derderian, G. J.; Barrie, J. D.; Aitchison, K. A.; Adams, P. M.; Mecartney, M. L. *J. Am. Ceram. Soc.* **1994**, *77*, 820.
(34) Lu, C. H.; Lo, S. Y.; Lin, H. C. *Mater. Lett.* **1998**, *34*, 172.
(35) Feng, S.; Li, G.; Li, L.; Li, X. *Rev. High Pressure Sci. Technol.* **1998**, *7*, 1362.
(36) Uchida, S.; Inoue, Y.; Fujishiro, Y.; Sato, T. *J. Mater. Sci.* **1998**, *33*, 5125.
(37) Komatsu, R.; Adachi, K.; Ikeda, K. *Jpn. J. Appl. Phys., Part 1* **2001**, *40*, 5657.
(38) Goh, G. K. L.; Lange, F. F.; Haile, S. M.; Levi, C. G. *J. Mater. Res.* **2003**, *18*, 338.
(39) Wu, Z. B.; Tsukada, T.; Yoshimura, M. *J. Mater. Sci.* **2000**, *35*, 2833.
(40) Wu, Z. B.; Tsukada, T.; Yoshimura, M. *J. Mater. Res.* **2000**, *15*, 1154.
(41) Goh, G. K. L.; Levi, C. G.; Lange, F. F. *J. Mater. Res.* **2002**, *17*, 2852.
(42) Lange, F. F. *Science* **1996**, *273*, 903.
(43) Chien, A. T.; Speck, J. S.; Lange, F. F.; Daykin, A. C.; Levi, C. G. *J. Mater. Res.* **1995**, *10*, 1784.
(44) Chien, A. T.; Sachleben, J.; Kim, J. H.; Speck, J. S.; Lange, F. F. *J. Mater. Res.* **1999**, *14*, 3303.
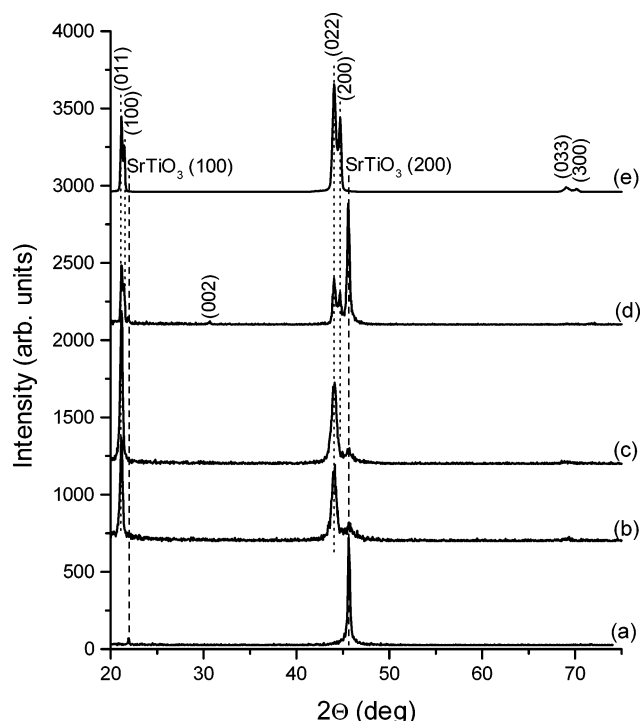(45) Chien, A. T.; Speck, J. S.; Lange, F. F. *J. Mater. Res.* **1997**, *12*, 1176.

Figure 1. XRD patterns of orthorhombic $KNbO_3$ films deposited hydrothermally on single-crystal $SrTiO_3$ (100) substrates at 200 °C (48 h) from aqueous solutions containing (a) 4.0 m KOH and 0.50 m Nb_2O_5; (b) 6.0 m KOH and 0.50 m Nb_2O_5; (c) 6.0 m KOH and 0.20 m Nb_2O_5; (d) 10.0 m KOH and 0.05 m Nb_2O_5; and (e) 10.0 m KOH and 0.50 m Nb_2O_5. Note absence of any deposits in (a), preferred (011) orientation of the $KNbO_3$ films in (b) and (c), and mixed (100)/(011) orientation of the $KNbO_3$ films in (d) and (e).

Experimental Procedure

Hydrothermal Synthesis of $KNbO_3$ Films. Niobium pentoxide (Nb_2O_5, purity 99.9%, Alfa Aesar, Ward Hill, MA) and potassium hydroxide (KOH, pellets, assay 85 wt %, Fisher Scientific, Pittsburgh, PA) were used to prepare precursors for hydrothermal synthesis of $KNbO_3$ films. The concentration of the reactants in the aqueous precursors ranged between 0.05 and 0.50 m for Nb_2O_5, and 2.0 and 14.0 m for KOH. It should be noted that all concentrations are expressed in molality (m), i.e. number of mols per 1 kg of H_2O. The $KNbO_3$ precursors were prepared in 100-mL PTFE bottles with screw caps, according to the following procedure. First, 6.60−46.20 g of KOH was fully dissolved in such quantities of de-ionized water to yield a total water content of 35−50 g. Following complete dissolution of the KOH in water, 0.465−6.645 g of Nb_2O_5 powders were added, as required by stoichiometry. Subsequently, the substrates, ultrasonicated earlier in isopropyl alcohol (assay min. 99%, histology grade, EM Science, Gibbstown, NJ) for 30 min and dried in air, were placed in the upper part of each bottle (below the solution level) using PTFE tubing as holders. The following single-crystal substrates were used in the hydrothermal experiments: (i) polished $SrTiO_3$ with (100) orientation (dimensions 5 mm × 5 mm × 0.5 mm, Coating and Crystal Technology, Inc., Kittanning, PA); (ii) polished $SrTiO_3$ (100) 1-in. wafers (Marketech International, Port Townsend, WA); and (iii) polished $LiTaO_3$ (001) ($\approx$5−10 mm × 5−10 mm × 0.4 mm pieces from a broken 3-in. wafer, Sawyer Crystal Systems, Inc., Conroe, TX).

(46) Suchanek, W. L.; Oledzka, M.; Mikulka-Bolen, K.; Pfeffer, R. L.; Lencka, M.; McCandlish, L.; Riman, R. E. *Proceedings of Fifth International Conference on Solvothermal Reactions (ICSTR)*, East Brunswick, New Jersey, July 22−26, 2002; 2002; p 159.
(47) Oledzka, M.; Lencka, M. M.; Pinceloup, P.; Mikulka-Bolen, K.; McCandlish, L. E.; Riman, R. E. *Chem. Mater.* **2003**, *15*, 1090.
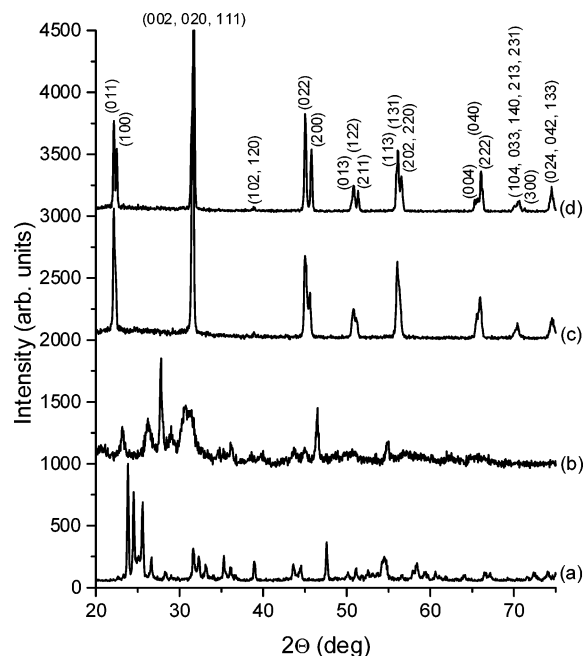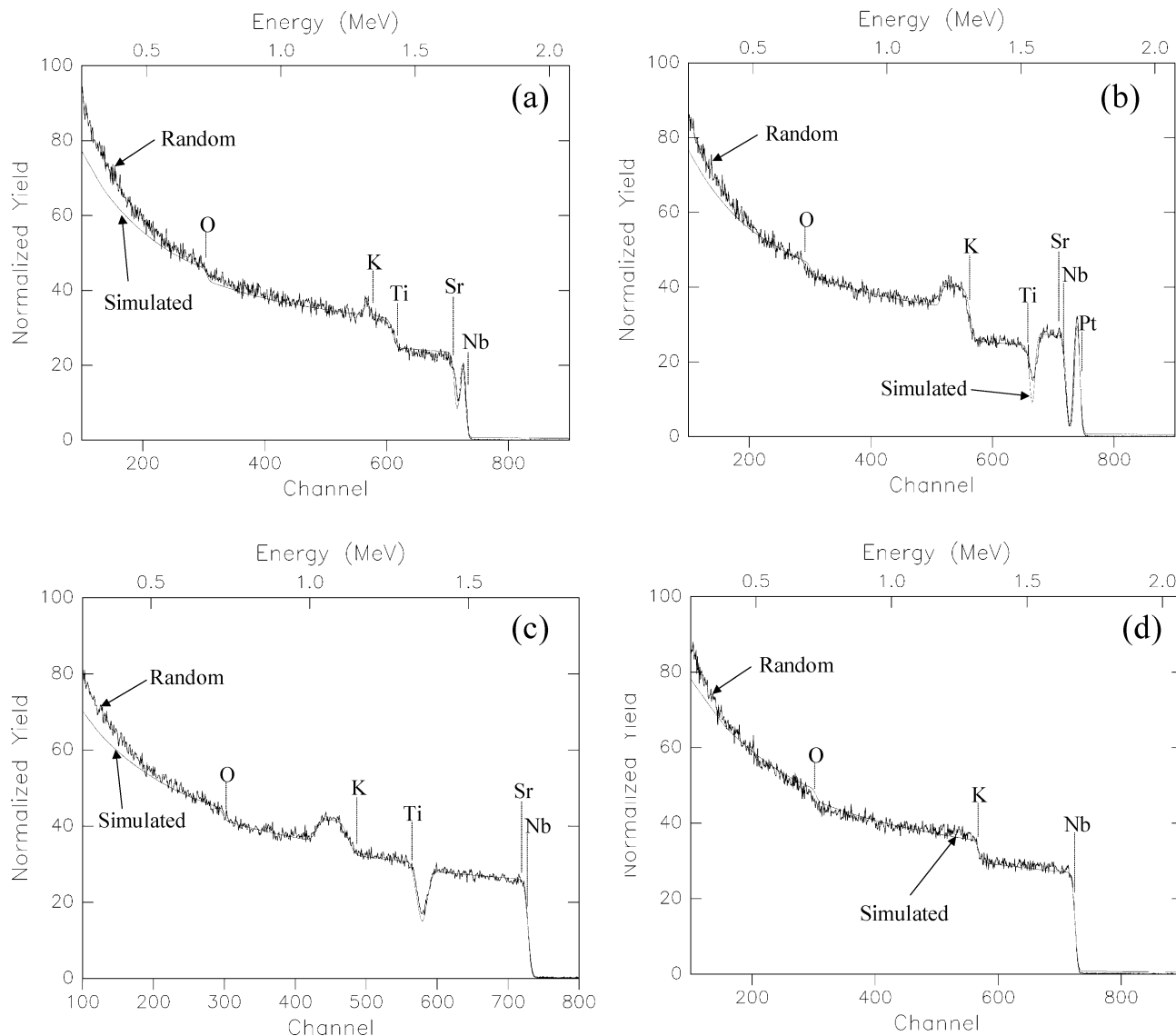

Figure 2. XRD patterns of the solid phases precipitated under hydrothermal conditions at 200 °C (48 h) simultaneously with the film deposition in the bulk of aqueous solutions with various chemical compositions: (a) no treatment; (b) 2.0 m KOH and 0.50 m Nb_2O_5; (c) 6.0 m KOH and 0.05 m Nb_2O_5; and (d) 10.0 m KOH and 0.50 m Nb_2O_5. The observed phases were: (a) Nb_2O_5 (unreacted powder); (b) $K_4Nb_6O_{17}$ (major phase); (c) and (d) orthorhombic $KNbO_3$.

The hydrothermal syntheses of $KNbO_3$ thin films were performed in autoclaves with a 13-in. internal diameter and internal length of 120 in. (manufactured by Autoclave Engineers, Erie, PA). In each experiment, 9−15 PTFE bottles containing the precursors and substrates were attached to a steel rack using steel wires. The PTFE bottles were closed tight using the screw caps, but all had capillary holes drilled through the caps (from the side) in order to allow pressure equilibration between the inside of the bottles and the internal parts of the autoclave. The rack with the attached PTFE bottles was placed inside the autoclave on a spacer, in such a way that it was positioned in the upper half of the autoclave. The bottom part of the autoclave was filled with de-ionized water to about half of the height of the spacer ($^1/_4$ of the autoclave volume). The autoclave was closed with a plug and three internal thermocouples were placed inside in order to measure temperatures in the upper and lower part of the rack with the bottles, as well as in the bottom section of the autoclave.

Most of the hydrothermal runs were carried out at the temperatures of 180 °C (48 h) or 200 °C (48 h). A very limited number of experiments was carried out also at 210 °C (48 h). The average measured heating rate in the temperature range of 20−210 °C was 0.48 °C/min. The corresponding pressures were the saturated vapor pressures of water at 180, 200, and 210 °C, i.e., 1.00, 1.55, and 1.91 MPa, respectively. The samples were cooled together with the autoclaves in an uncontrolled fashion.

After each synthesis run and opening the autoclave, the PTFE bottles with samples were removed from the rack. The solutions with precipitates (if any) were collected and stored for future reference. Some of the precipitates were washed several times with de-ionized water and subsequently dried. The films deposited on the substrates were removed from the holders, placed in glass beakers and subjected to ultrasonic cleaning in de-ionized water for 20 min and subsequently in isopropyl alcohol for 10 min. The substrates with films were dried overnight at room temperature.

Characterization of the Materials. Phase composition and crystallographic orientation of all synthesized films and selected powder precipitates was characterized by X-ray dif-

Figure 3. Random and simulated RBS spectra of typical KNbO$_3$ films deposited hydrothermally on single-crystal SrTiO$_3$ (100) substrates at 200 °C (48 h) from aqueous solutions containing: (a) 4.0 m KOH and 0.05 m Nb$_2$O$_5$; (b) 6.0 m KOH and 0.20 m Nb$_2$O$_5$; (c) 6.0 m KOH and 0.20 m Nb$_2$O$_5$ (coated twice); and (d) 10.0 m KOH and 0.50 m Nb$_2$O$_5$. Thickness of the films was (a) 45 nm; (b) 270 nm; (c) 725 nm; and (d) over 3.5 μm. In (b) the first sharp peak is derived from a 6-nm-thick palladium layer which was sputtered on the film surface.

fraction using an Advanced Diffraction System X1 diffracto-meter (XRD, Scintag Inc.) using Cu Kα radiation, in the 2θ range between 20 and 75° with a 0.05° step size and 0.3−0.7-s count time. The chemical identity and orientation of the materials was determined by comparing the experimental XRD patterns to standards compiled by the Joint Committee on Powder Diffraction and Standards (JCPDS), i.e., card 35-0734 for SrTiO$_3$, 29-0836 for LiTaO$_3$, 71-0946 for orthorhombic KNbO$_3$, 08-0212 for cubic KNbO$_3$, 28-0788 for K$_2$Nb$_6$O$_{16}$, and 21-1295 for K$_4$Nb$_6$O$_{17}$.

Chemical composition and thickness of selected films were measured by Rutherford backscattering (RBS). For this pur-pose, the film samples were attached to the stage of a goniometer in the beamline of a 1.7-MV tandem pelletron accelerator (model 5SDH, National Electrostatics Corporation, Middletown, WI). The 2.00-MeV He^{2+} ion beam was used to obtain the RBS spectra. The beam was collimated to a rectangular spot approximately 1 mm × 1 mm. The RBS data were recorded over 800 channels. Compositional and thickness analysis of the films were done by matching the data to simulation spectra generated with the RUMP RBS analysis software package.[48,49] To estimate the degree of crystalline order, selected samples were measured using ion channeling. This involved measuring the yield of backscattered ions (in

an energy window corresponding to backscattering events just beneath the films' surface) as a function of rotation angle. The resulting angular scan showed sharp dips in the yield at angles characteristic of crystalline plane directions. Subsequently, RBS spectra in the entire energy range were recorded in the channels with minimum yields and compared to the random spectra.

The morphology of selected synthesized KNbO$_3$ films was examined using scanning electron microscopy (SEM, model S-4500, Hitachi, Japan) at 5-kV accelerating voltage. The KNbO$_3$ films on the substrates were mounted directly to the metal sample holders using a conductive carbon tape. All film samples were sputtered with thin conductive layers of plati-num prior to the SEM examination.

Results

Hydrothermal Deposition of KNbO$_3$ Films on SrTiO$_3$ (100) Substrates. A wide range of orthorhom-bic KNbO$_3$ films was synthesized under hydrothermal

(48) Doolittle, L. R. *Nucl. Inst. Methods* **1985**, *B9*, 334.
(49) Doolittle, L. R. *Nucl. Inst. Methods* **1986**, *B15*, 227.

conditions on $SrTiO_3$ (100) substrates during the course of this work. Typical XRD patterns of the deposited films are shown in Figure 1. No other XRD peaks except for those derived from either $SrTiO_3$ or $KNbO_3$ phases were detected. The films prepared at lower concentrations of KOH, which ranged between 4.0 and 6.0 m, were single-phase $KNbO_3$ with (011) orientation. Only the (011) and (022) reflections were visible in the XRD patterns (Figure 1b and c), in addition to the (100) and (200) reflections from the $SrTiO_3$ substrate (Figure 1a). At the KOH concentrations above 6.0 m, the films exhibited mixed (100)/(011) orientation, as demonstrated by presence of both (100), (200), (300), and (011), (022), (033), XRD peaks (Figure 1d and e). Orientation of the $KNbO_3$ films appeared to be independent of the Nb_2O_5 concentration in the investigated 0.05–0.50 m range.

Simultaneously with the film deposition, white solid precipitates were formed in almost all solutions of aqueous precursors used for the $KNbO_3$ films synthesis. At KOH concentration of 2.0 m only $K_4Nb_6O_{17}$ phase was detected by XRD (Figure 2b). At higher KOH concentrations, only the orthorhombic $KNbO_3$ phase crystallized in the bulk of the coating solutions (Figure 2c and d).

The synthesized $KNbO_3$ films had thicknesses ranging between 45 nm and >3.5 μm, as measured by the RBS technique. The RBS spectra confirmed high purity and stoichiometry of the deposited $KNbO_3$ films. Figure 3 shows RBS spectra representative of orthorhombic $KNbO_3$ films, with different thicknesses and crystallographic orientations. An RBS spectrum of a 45-nm-thick $KNbO_3$ film with (011) orientation is shown in Figure 3a. Figure 3b and c show RBS spectra of (011) oriented $KNbO_3$ films with thicknesses of 270 and 725 nm, respectively. A typical RBS spectrum of a thick (>3.5 μm) $KNbO_3$ film with a mixed (100)/(011) orientation is presented in Figure 3d. The recorded random RBS spectra were in a very good agreement with the calculated ones, indicating stoichiometric $KNbO_3$ composition and high purity of the films. They did not indicate any significant interdiffusion between the $KNbO_3$ films and the $SrTiO_3$ substrates.

Epitaxial relationship between the $SrTiO_3$ (100) substrate and the hydrothermally synthesized $KNbO_3$ (011) films has been demonstrated by the RBS ion channeling measurements. RBS ion channeling measurements of selected $KNbO_3$ (011) films indicated very high level of the film orientation. A proper angle for axial channeling could be calculated from angular scans, and an RBS spectrum was measured with the sample aligned at those angles. For typical $KNbO_3$ (011) films, comparison of the aligned ion channeling and random RBS spectra (Figure 4) shows that the films exhibit a very high level of orientation and are highly aligned with respect to the $SrTiO_3$ (100) substrate.

Microstructures of the $KNbO_3$ films further confirmed their high level of 3D orientation. Figure 5 shows representative microstructures of the $KNbO_3$ films. $KNbO_3$ (011) films with thickness ranging between 45 nm and 1.28 μm exhibited microstructures without clearly defined grains or grain boundaries (Figure 5a–c). They consisted of multiple layers of small building blocks (10-nm size), which often formed quasi-dendritic/fractal-like structures. Conversely, the films with the
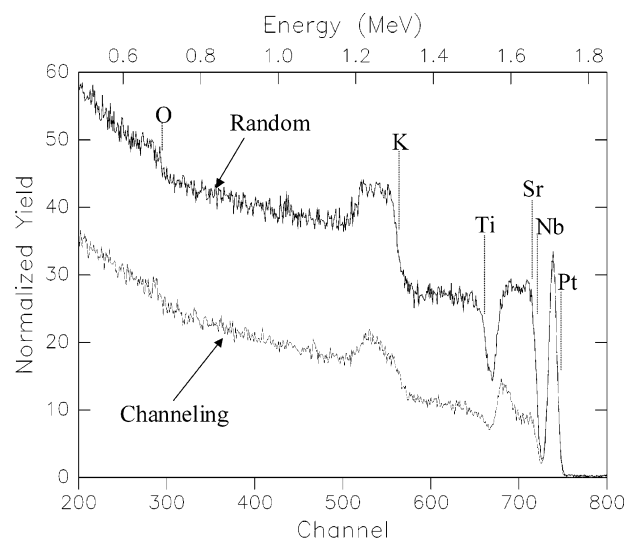

Figure 4. Random and ion channeling RBS spectra of the $KNbO_3$ (011) film deposited hydrothermally on single-crystal $SrTiO_3$ (100) substrates at 200 °C (48 h) from aqueous solutions containing 6.0 m KOH and 0.20 m Nb_2O_5. The first sharp peak with the same intensity in both RBS spectra is derived from a 6-nm-thick palladium layer which was sputtered on the film surface.

thickness of several μm were very rough and consisted of highly textured columnar grains, as shown in Figure 5d.

In most cases, the synthesized $KNbO_3$ films were very uniformly distributed on the $SrTiO_3$ substrates, including 1-in. wafers, and covered the entire substrate surface. All $KNbO_3$ films with 45 nm to 1.28 μm thickness were optically transparent irrespective of the orientation, whereas the $KNbO_3$ films thicker than 3.5 μm were milky and translucent. Neither cracks nor peeling-off were observed in the synthesized $KNbO_3$ films, except for a few samples with the highest film thickness (>3.5 μm). Occasionally, inclusions of $KNbO_3$ particles were incorporated in the films synthesized at 200–210 °C.

Hydrothermal Deposition of $KNbO_3$ Films on $LiTaO_3$ Substrates. $KNbO_3$ films were successfully deposited on $LiTaO_3$ (001) wafers at 180–200 °C at high KOH concentrations between 10 and 14 m. Typical XRD patterns of the $KNbO_3$ films on $LiTaO_3$ are shown in Figure 6. Some of the films appear to be orthorhombic with (100) orientation, as shown in Figure 6c. XRD patterns of other films indicate either $KNbO_3$ polycrystalline films with random orientation and possible cubic symmetry or formation of multidomain orthorombic $KNbO_3$ having domains with different crystallographic orientations (Figure 6b).

Microstructure of a selected $KNbO_3$ film on $LiTaO_3$ substrate is shown in Figure 7. The film microstructure appears to be polycrystalline but with a high level of orientation. It is worth mentioning that a very few shallow etch pits were observed on the $LiTaO_3$ substrates during the deposition of $KNbO_3$ films.

Discussion

Regions of deposition of the $KNbO_3$ films on both $SrTiO_3$ and $LiTaO_3$ substrates as functions of the temperature, in the 180–200 °C range, and reactants'
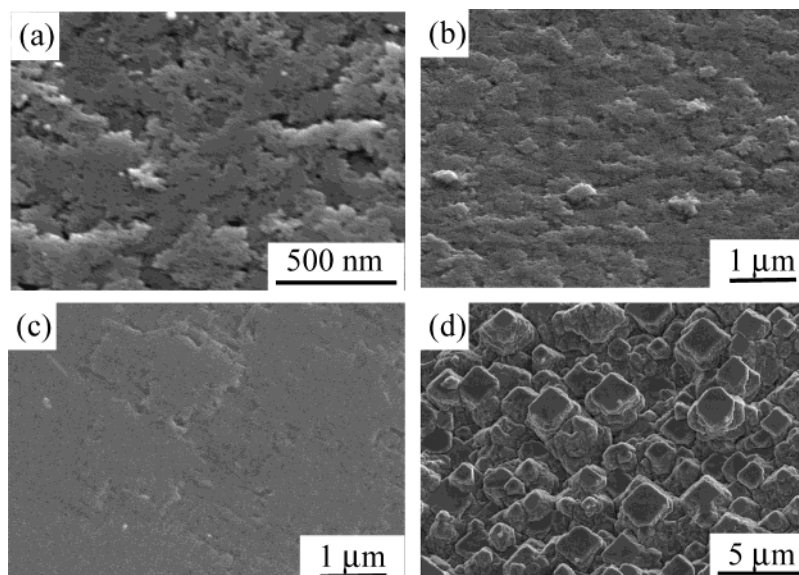
Figure 5. SEM photographs of orthorhombic KNbO$_3$ films deposited hydrothermally on single-crystal SrTiO$_3$ (100) substrates from aqueous solutions containing (a) 6.0 m KOH and 0.50 m Nb$_2$O$_5$ (200 °C, 48 h); (b) 6.0 m KOH and 0.20 m Nb$_2$O$_5$ (200 °C, 48 h); (c) 6.0 m KOH and 0.20 m Nb$_2$O$_5$ (210 °C, 48 h); (d) 10.0 m KOH and 0.50 m Nb$_2$O$_5$ (200 °C, 48 h).
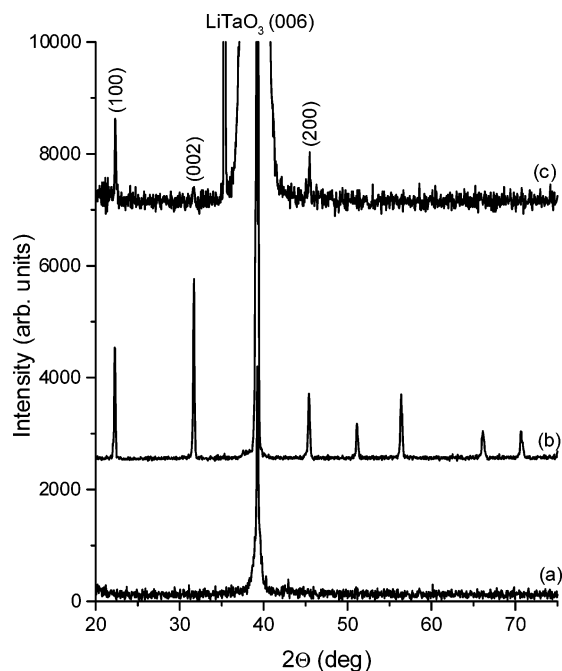

Figure 6. XRD patterns of KNbO$_3$ films deposited hydrothermally on single-crystal LiTaO$_3$ (001) substrates at 180 °C (a and c) and 200 °C (b) for 48 h from aqueous solutions containing (a) 6.0 m KOH and 0.20 m Nb$_2$O$_5$ (no film deposition); (b) 14.0 m KOH and 0.20 m Nb$_2$O$_5$; and (c) 10.0 m KOH and 0.20 m Nb$_2$O$_5$.

Figure 7. SEM photographs of a KNbO$_3$ film deposited hydrothermally on single-crystal LiTaO$_3$ (001) substrate at 180 °C (48 h); reactants concentration: 10.0 m KOH and 0.20 m Nb$_2$O$_5$.

concentrations are summarized in Figure 8. In general, higher KOH concentrations favored formation of the KNbO$_3$ films. The boundaries of the stability regions of the KNbO$_3$ films were around 5 m KOH at 200 °C and 7−9 m KOH at 180 °C. In addition, at the boundary KOH concentrations, the KNbO$_3$ films started forming at very low Nb$_2$O$_5$ concentration, whereas at higher Nb$_2$O$_5$ concentrations no deposition of any kind was observed. Because of the very limited number of synthesis experiments conducted at 210 °C, stability regions of the KNbO$_3$ films at this temperature were not established.
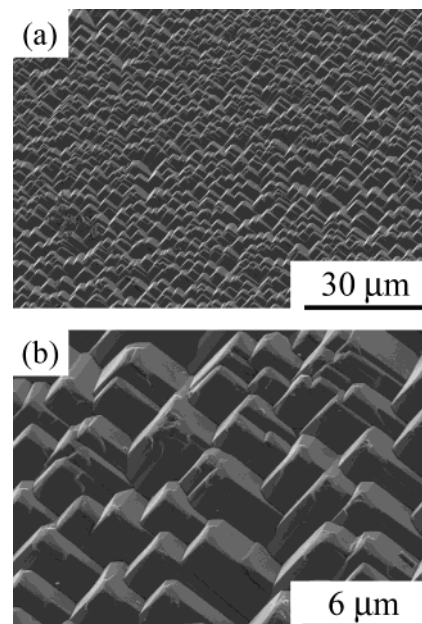
Although no attempts to grow orthorhombic KNbO$_3$ films below 180 °C were undertaken in this work, it is quite possible that the films could be deposited under such conditions. However, the films deposited at 180 °C, particularly those which were synthesized at lower concentrations of the reactants, tend to be much thinner that the corresponding films synthesized at 200 °C. Therefore, it seems that even if the deposition of orthorhombic KNbO$_3$ films were possible at temperatures lower than 180 °C, it would probably require rather high KOH and Nb$_2$O$_5$ concentrations with a possibility of producing very thin films and/or incomplete substrate coverage.

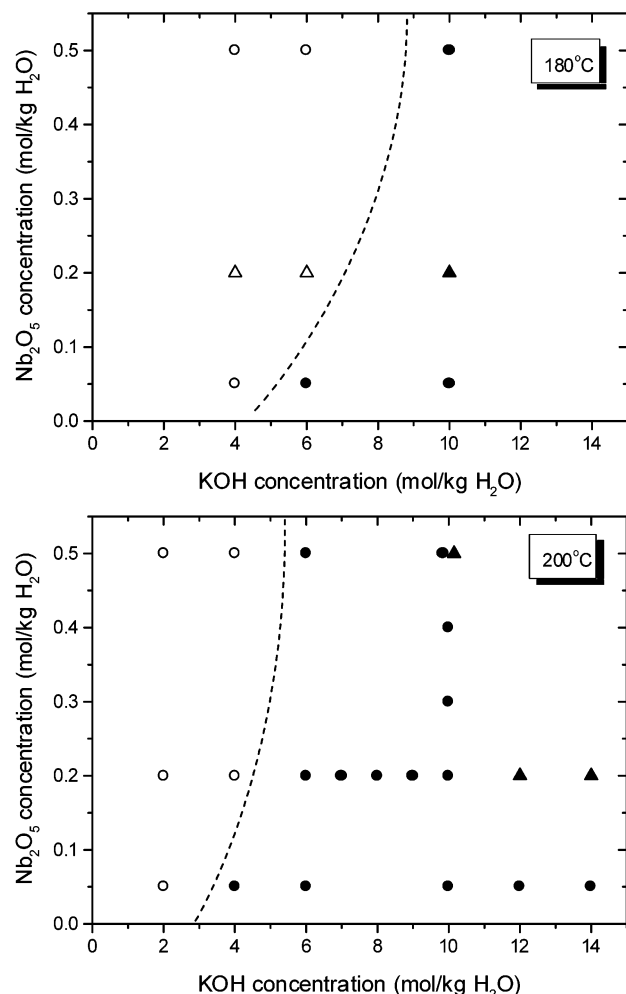The morphology of the KNbO$_3$ films deposited on SrTiO$_3$ substrates was found to be a function of the KOH

Figure 8. Maps showing deposition of KNbO$_3$ films under hydrothermal conditions at 180 and 200 °C for 48 h: open symbols denote no film formation; solid symbols denote formation of KNbO$_3$ films; circles represent deposition (or attempted deposition) of orthorhombic KNbO$_3$ films on SrTiO$_3$ (100) substrates, and triangles represent deposition (or attempted deposition) of KNbO$_3$ films on LiTaO$_3$ (001).

concentration. Single crystal-like orthorhombic KNbO$_3$ films with (011) orientation and 45 nm to 1.28 μm thickness were formed at KOH concentrations of 4.0–6.0 m, almost irrespectively of the Nb$_2$O$_5$ concentration. The (011) orientation with respect to the (100) orientation of the SrTiO$_3$ substrate was already observed in other works.[50] Single crystallographic orientation of the KNbO$_3$ films in conjunction with the low synthesis temperature may indicate single-domain nature of the films. However, existence of domains in the KNbO$_3$ film cannot be easily distinguished by XRD.[50] The morphology of these films resembled layered growth of nm-size clusters forming dendritic/fractal-like microstructures. Similar microstructures were observed earlier in the case of epitaxial Pb(Zr$_x$Ti$_{1-x}$)O$_3$ (PZT) films deposited under hydrothermal conditions.[46] This kind of microstructure is typical for growth of single crystals from molecular clusters[51] strongly suggesting single-crystal nature of the epitaxial KNbO$_3$ (011) films. At the KOH concentrations of 7.0 m and higher, the KNbO$_3$ films

exhibited mixed (100)/(011) orientation. With increasing concentrations of both reactants, the films were initially covered with islands and subsequently with uniform and very thick layers of strongly textured orthorhombic KNbO$_3$. The mixed crystallographic orientation appears to be associated with the thickest films, i.e., >3.5 μm, and could be ascribed to multidomain formation as a relaxation mechanism of thermoelastic stresses, which increase within the film with increasing thickness.[52]

The described hydrothermal synthesis of epitaxial orthorhombic KNbO$_3$ films has the following advantages as compared to the previously used techniques. The deposition technique utilizes low-temperature aqueous solutions and simple reactants (Nb$_2$O$_5$ powder, KOH). Because the synthesis can be accomplished below the orthorhombic–tetragonal phase transition temperature of 225 °C, orthorhombic KNbO$_3$ films with a single crystallographic orientation, and probably also single-domain structure, can be formed in a well-defined range of synthesis conditions, which have been established for the first time in this work. The films can be uniformly distributed on the entire substrate area without stirring, exhibit high stoichiometry, and do not show evidence of interdiffusion or chemical reaction at the film/substrate interface, which is often associated with the high-temperature processing. In addition, the KNbO$_3$ is a lead-free material, which, together with excellent piezoelectric and optical properties of the KNbO$_3$ film, implies many optical, surface acoustic wave, and other applications.

Hydrothermal deposition of KNbO$_3$ films is, of course, not limited to substrates such as SrTiO$_3$ and LiTaO$_3$. Capability of the hydrothermal method to deposit films with different orientations, morphologies, and chemical compositions on various substrates has been demonstrated in many works.[42,53,54] It is also worth mentioning that KNbO$_3$ is known to form a variety of solid solutions, for example (Na,K)NbO$_3$,[55] (Li,K)NbO$_3$,[56] K(Nb,Ta)O$_3$,[32] (K$_{0.5}$Bi$_{0.5}$)TiO$_3$–KNbO$_3$,[57] BaTiO$_3$–KNbO$_3$,[58] and PZN–KNbO$_3$–PZT,[59] etc. KNbO$_3$ can be also doped with a variety of ions, such as Li$^+$, Ba^{2+}, Sm^{3+}, Ce^{4+}, and V^{5+}, etc.[60] All these materials exhibit a variety of attractive piezoelectric, ferroelectric, and electrooptic properties, which can be tailored by properly adjusting their chemical compositions. Most important among the principal features of the hydrothermal synthesis is that it allows an easy synthesis of a variety of solid solutions in the form of films. Good examples are PZT films[42] or (Ba,Ca,Sr)(Mo,W)O$_3$ films.[61] Therefore, the results of the present work strongly imply the possibility of hydrothermal deposition of thin films of a variety of solid-solution compositions based on KNbO$_3$, particularly

(50) Gopalan, V.; Raj, R. *J. Am. Ceram. Soc.* **1996**, *79*, 3289.
(51) Askhabov, A. M. *Syktyvkar Mineralogical Collection* **2001**, *30*, 14.

(52) Ohring, M. *The Materials Science of Thin Films*; Academic Press: New York, 1992.
(53) Yoshimura, M.; Suchanek, W. *Solid State Ionics* **1997**, *98*, 197.
(54) Suchanek, W. L.; Yoshimura, M. *J. Am. Ceram. Soc.* **1998**, *81*, 2864.
(55) Egerton, L.; Dillon, D. M. *J. Am. Ceram. Soc.* **1959**, *42*, 438.
(56) Zhang, H. X.; Kam, C. H.; Zhou, Y.; Han, X. Q.; Cheng, S. D.; Chan, C. Y.; Lam, Y. L. *J. Mater. Res.* **2001**, *16*, 3609.
(57) Wada, T.; Toyoike, K.; Imanaka, Y.; Matsuo, Y. *Jpn. J. Appl. Phys., Part 1* **2001**, *40*, 5703.
(58) Ravez, J.; Simon, A. *Solid State Sci.* **1999**, *1*, 25.
(59) Takenaka, T.; Satou, M.; Nakata, K.; Sakata, K. *Ferroelectrics* **1992**, *128*, 67.
(60) Ding, S.; Shen, J. *J. Am. Ceram. Soc.* **1990**, *73*, 1449.
(61) Cho, W.-S.; Yoshimura, M. *J. Appl. Phys.* **1998**, *83*, 518.

because many of the materials mentioned above can be synthesized under mild hydrothermal conditions.

Conclusions

KNbO$_3$ thin films were deposited on single-crystal oxide substrates, including 1-in. wafers, by hydrothermal epitaxy at 180−210 °C using simple reactants. Well-defined ranges of synthesis conditions for the KNbO$_3$ films in terms of temperatures and reactants concentrations were established. The KNbO$_3$ films with 45 nm to 3.5 μm thickness were uniformly distributed on the entire substrate area without stirring, exhibited high stoichiometry, and did not show evidence of interdiffusion or chemical reaction at the film/substrate interface. Neither cracks nor peeling-off were observed in most cases. High levels of crystallographic orientation and microstructures of some of the films suggest single-crystal growth. The low synthesis temperatures, which are below the 225 °C phase transition temperature of KNbO$_3$, allowed synthesis of pure orthorhombic epitaxial KNbO$_3$ films with (011) orientation and probably single-domain that are expected to exhibit improved properties as compared to the films prepared by high-temperature processing.

CM034952Q